# Interference effects in spontaneous two-photon parametric scattering from two macroscopic regions

A. V. Burlakov,[1] M. V. Chekhova,[1] D. N. Klyshko,[1] S. P. Kulik,[1] A. N. Penin,[1] Y. H. Shih,[2] and D. V. Strekalov[2]
[1]*Physics Department, Moscow State University, Moscow, Russia*
[2]*Physics Department, University of Maryland, Baltimore County, Baltimore, Maryland 21228*
(Received 6 March 1997)

Two types of interference were observed using two-photon spontaneous parametric radiation from two nonlinear interaction regions. Two experimental setups analogous to the Young and Mach-Zehnder interferometers were used. An interesting feature of the two-photon Young interference is the opposite conditions for its observation by two different methods: by measuring intensity of light at a single frequency and by measuring correlation of intensities at two conjugated frequencies (method of coincidences). Two-photon Mach-Zehnder interference resembles the Ramsey method of separated fields, which is used in beam spectroscopy. A simple macroscopic quantum model agrees well with the experimental results and enables their interpretation in terms of ''biphotons'' carrying information about the pump phase. [S1050-2947(97)03210-1]

PACS number(s): 42.50.Ct, 42.50.Hz, 42.50.Ar

## I. INTRODUCTION

The parametric scattering effect (PS), or spontaneous parametric down-conversion (SPDC), is the most simple and effective source of nonclassical light. This effect can be interpreted as a spontaneous decay of pump photons with frequency $\omega_p$ to pairs of photons with frequencies $\omega$ and $\omega'$ ($\omega,\omega'<\omega_p$) according to the scheme $\hbar\omega_p \rightarrow \hbar\omega+\hbar\omega'$. The scattered field is represented by pairs of photons (''*biphotons*'') correlated in frequency and propagation direction. Phenomenologically, this field is described using the macroscopic nonlinear susceptibility $\chi$ of the substance and quantizing the macroscopical scattered field. The pump is usually a laser field, which is considered classical. PS is observed in transparent birefringent crystals with a large $\chi$ and without a center of symmetry (as lithium niobate or KDP).

The PS attracts great attention in connection with the demonstration of Bell's inequality violation [1–3] and with the possible realization of quantum cryptography and quantum computing [4,5]. Applications of PS are also known in spectroscopy [6], metrology [5–7], and the measurement of group delay times [8,9].

This work is devoted to the study of coherent properties of PS field and of ways to construct a biphoton field. The experiments carried out confirm that the information about the pump phase can be transmitted with the help of biphotons.

In the case of a uniform crystal and a plane monochromatic pump wave, spontaneous emission of photon pairs occurs mostly in the directions determined by the phase matching conditions $\omega+\omega'-\omega_p=0$ and $\vec{\Delta}\equiv\vec{k}+\vec{k}'-\vec{k}_p=0$ (here $\vec{k}$ are the wave vectors inside the crystal). These equalities, called phase matching conditions, together with the crystal dispersion $\omega(\vec{k})$ determine the specific shape of the frequency-angular spectrum of PS, that is, the probability $P(\vec{k},\vec{k}')$ of a photon pair emission into the conjugate modes $\vec{k}$ and $\vec{k}'$. The field of given frequency $\omega$ is emitted mostly at a definite angle $\theta=\theta(\omega)$ between $\vec{k}$ and $\vec{k}_p$. One of the conjugated modes $(\vec{k},\vec{k}')$ (with wave vector $\vec{k}$ and frequency $\omega$) is called the signal, the other (with wave vector $\vec{k}'$ and frequency $\omega'=\omega_p-\omega$) is called the idler. Two basic methods to study PS are possible: by a single detector, when only properties of the signal modes with frequency $\omega$ are observed, and by two detectors, using a coincidence circuit and measuring the intensity correlation in two conjugated modes. As one of the frequencies (e.g., $\omega'$) decreases and approaches the region of strong IR absorption and dispersion, the PS gradually turns into the Raman scattering of light by polaritons (optical phonons). The border between these two processes can be set by the condition $\alpha' l'=1$, where $\alpha'$ is the absorption coefficient for the idler wave and $l'$ is the length of the scattering region along $\vec{k}'$.

The probability of detecting a biphoton has the form $P(\vec{k},\vec{k}')=|F(\vec{k},\vec{k}')|^2$; see [11]. The function $F(\vec{k},\vec{k}')$ can be viewed as a *two-photon wave packet* or a state vector of the biphoton in the momentum space $(\vec{k})\otimes(\vec{k}')$. The Fourier transform of $F(\vec{k},\vec{k}')$ may be interpreted as some effective biphoton field in the space $(\vec{r},t)\otimes(\vec{r}',t')$, which defines the probability to detect a pair of photons at some point of this space. Spontaneous scattering is closely related to induced one [10,11]: let, for instance, a coherent field be fed to the input of the idler mode $\vec{k}'$, so that $\langle a_{\vec{k}'}\rangle\neq 0$; then the output signal $\langle a_{\vec{k}}\rangle=F(\vec{k},\vec{k}')\langle a_{\vec{k}'}\rangle$. Therefore, $F(\vec{k},\vec{k}')$ plays the role of the scattering matrix for the whole nonlinear region $V$ (in our case, it consists of two interaction regions excited coherently by a common pump).

If the interaction region $V$ has inhomogeneous linear and/or nonlinear optical properties or contains reflecting surfaces, the condition $\vec{\Delta}=\vec{k}+\vec{k}'-\vec{k}_p=0$, which is usually interpreted as the momentum conservation law for photons and which defines the specific shape of the frequency-angular spectrum of PS, can be modified. Then the frequency-angular spectrum displays an additional structure.

Effects of reflections that cause multiple interactions of waves in a single crystal were studied [12–14]. In Ref. [12],

 

multiple reflections from the parallel sides of the crystal and also absorption $\alpha'$ at the idler frequency were taken into account. If the pump is intense enough, reflections can lead to the enhanced regime, that is, the parametric generation of light. In Ref. [13], a periodic variation of biphoton emission intensity (in fixed directions) was observed in two conjugated modes as either one of three mirrors, reflecting the parametric radiation and pump back to the crystal, was moved. In Ref. [14], PS was observed from a thin nonlinear layer parallel to $\vec{k}_p$. Its frequency-angular spectrum was found to be periodically modulated due to multiple full internal reflections of the idler waves.

It is well known that the spectrum of usual spontaneous radiation by atoms and molecules significantly alters if the surrounding field configuration and its mode density is modified by external mirrors. The specific feature of the experiments described below is monitoring the spectrum of two-photon spontaneous radiation without any such mirrors but because of the interference of the spontaneous fields generated in two regions separated in space by a macroscopic distance.

The goal of this work is to study interference and diffraction of the PS light due to the nonuniform distribution of the quadratic nonlinearity $\chi(\vec{r})$ or to a slow variation of the pump amplitude $E_p(\vec{r})$ in the region of interaction. The local amplitude of three-waves interaction is characterized by the effective field $f(\vec{r},\vec{k},\vec{k}')\equiv\chi(\vec{r})E_p^*(\vec{r})\exp(i\vec{\Delta}\cdot\vec{r})$ (considering only linear approximation in $\chi E_p$). The frequency-angular spectrum of PS is determined by the integral

$$F(\vec{k},\vec{k}')\equiv\int_V f(\vec{r},\vec{k},\vec{k}')d^3r.$$

In the simplest case of a uniform crystal, this results in

$$F(\vec{k},\vec{k}')\propto\int_V\exp(i\vec{\Delta}\cdot\vec{r})d^3r\propto\delta_V^{(3)}(\vec{\Delta}),\qquad(1.1)$$

where $\delta_V^{(3)}(\vec{\Delta})$ is a function with a sharp ''resonant'' maximum at $\vec{\Delta}=0$ and the width determined by the dimensions of the region $V$. If, for example, the pump field inside the nonlinear crystal is a converging spherical wave then the spontaneous radiation observed by the method of photocounts coincidences may be said to focus in two points. The coordinates of the points are related to the pump wave-fronts curvature according to the rules of geometric optics for a spherical mirror [15]. A similar effect was observed by placing a collecting lens in front of the signal detector [16]. In the experiments of another type described below, the spatial nonuniformness of the interaction is due to the apertures placed in front of the crystal (Sec. II) or by two subsequent crystals separated by a linear medium (Sec. III).

Interference of intensities in the PS field spontaneously emitted by two (or more) coherently pumped crystals has been previously analyzed in [17–19]. Several types of interference in two-crystal cases were observed by Mandel and co-workers [20]; a general phenomenological description of those effects and their relation to induced ones has been shown [21]. These experiments, as well as PS in a multidomain crystal [22], may be formally described by spatially-

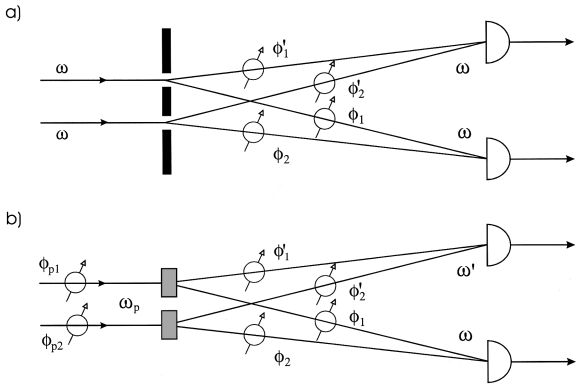


FIG. 1. Linear (a) and nonlinear (b) Young interferometers. The circles with arrows denote phase rotators at a single frequency (a) and at frequencies $\omega_p,\omega,\omega'$ (b).

nonuniform distribution of nonlinearity $\chi(\vec{r})$. In the case of several crystals (or domains), the total probability amplitude is $F=\Sigma_n F_n\exp(i\Delta\phi_n)$, where $n$ is the number of a specific crystal (or domain) and $\Delta\phi_n\equiv\phi_n+\phi_n'-\phi_{pn}$ is an additional (and adjustable) phase shift of the three waves. For example, for two domains $F=F_1+F_2\exp(i\Delta\phi)$, so that $|F|^2$ contains the interference term $2\,\mathrm{Re}[F_1^*F_2\exp(i\Delta\phi)]$. In the experiments [22], each two neighboring domains had opposite signs of $\chi$, which corresponded to the additional phase shift $\Delta\phi_n\rightarrow\Delta\phi_n+\pi$.

Experiments with two crystals were considered [3,17,23]. It is noteworthy that subsequent scattering in several crystals can be used to prepare two-photon field in an arbitrary polarization state [19], which may be of practical interest for information transmission [24].

There are two basic schemes analogous to the Young and Mach-Zehnder interferometers for the observation of biphoton fields interference (Figs. 1 and 2). Those schemes may be called nonlinear Young and Mach-Zehnder interferometers. In these schemes, interference of amplitudes (that is, the phase dependence of intensity) can be observed by either one of two detectors. Moreover, the degree of correlation between photocurrents of two detectors reveals interference of intensities. Visibilities of these two types of interference, which we respectively call interference of the second and fourth order, can be different. Moreover, as will be shown

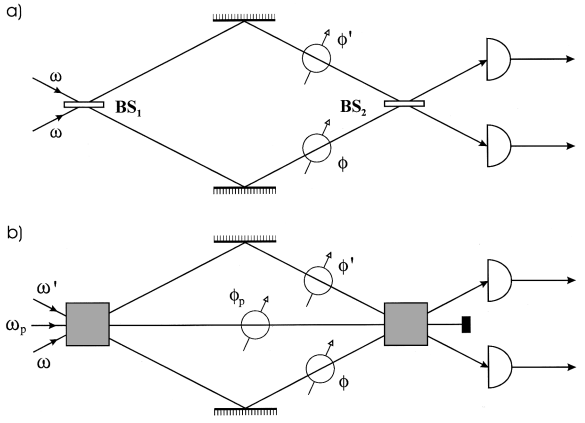


FIG. 2. Linear (a) and nonlinear (b) Mach-Zehnder interferometers.

later, conditions for their observation may be mutually exclusive. The scheme in Fig. 2(b) is analogous to Ramsey's method of separated fields in beam spectroscopy [18].

In the scheme 2(b), the interference pattern observed by both methods depends on the phase delays in the three arms of the interferometer: $\Delta\phi=\phi+\phi'-\phi_p$, and hence the effect can be considered as a three-frequency interference. In Fig. 1(b), the phase of the interference of amplitudes is $\Delta\phi=\phi_{12}-\phi_{p\,12}$, and the phase of the interference of intensities is $\Delta\phi=\phi_{12}+\phi'_{12}-\phi_{p\,12}$ ($\phi_{12}\equiv\phi_1-\phi_2$, and so on). Therefore, interference of intensities observed in the correlation between two detectors' photocurrents depends on the *sum* of optical paths $\phi+\phi'$ for the signal and idler waves. This is a specific feature of the interference of intensities observed using PS.

The effects discussed here have induced analogues, when the role of vacuum fluctuations is played by real coherent intense fields $\vec{k}$ and/or $\vec{k}'$ at the input of the scheme. Such an experiment was performed [25] using two crystals. An induced version of the scheme 2(b) is considered [26] and called the SU(1,1) interference. Theoretical descriptions of the spontaneous and induced processes are closely connected and have no principal distinctions [8,21]. Hence, spontaneous interference effects have close classical analogs. To describe such effects in terms of classical theory, it is sufficient to add a ''half photon'' in each input mode of the optical system, and to subtract them from the output modes [8,21]. Therefore, we can envision spontaneous effects as caused by vacuum fluctuations of the field surrounding the nonlinear crystals. In the presence of the pump, the crystals ''actualize'' these fluctuations and make them observable. Spatial and frequency spectra of the vacuum noise are unlimited, but the phase matching condition $\vec{\Delta}_{\vec{k}}=0$ selects from them two narrow bands called the tuning curves $\theta(\omega)$ and $\theta'(\omega)$. The tuning curves link the frequency $\omega$ and the scattering angles $\theta,\theta'$ together. All ''two-photon'' interference experiments can be in principle reproduced in the induced (i.e., classical) regime by supplying real noise fields of high intensity ($N\gg 1/2$) with frequencies $\omega$ and $\omega'$ to the input of the optical scheme, and performing analog detection. However, the essential difference will be a lower visibility of the observed intensity interference.

In both schemes in Figs. 1(b) and 2(b), spontaneous radiation is suppressed at some frequencies and angles and enhanced at others due to the existence of the second crystal. At first glance, this effect seems to be paradoxical, especially in the scheme with subsequently placed sources [Fig. 2(b)]: it is not clear how the first crystal (the left one) can suppress or enhance spontaneous radiation from the second crystal. Spontaneous processes in spatially separated points might seem to be independent, so the intensities should add up rather than the amplitudes. The paradox is formally resolved by taking into account that both crystals spontaneously radiate into some pair of output modes $(\vec{k},\vec{k}')_{\rm out}$ under the influence of vacuum fluctuations in the same initial modes $(\vec{k},\vec{k}')_{\rm in}$, so the spontaneous fields are mutually coherent. Also note that different interesting examples of the fourth order interference and diffraction using PS have been observed [27].

In the following Secs. II and III, simple models are described that explain PS in the schemes of Figs. 1(b) and 2(b), respectively. In Sec. IV, the actual experiments are described.

## II. THREE-FREQUENCY YOUNG'S INTERFEROMETER

The phenomenological description of PS can be based on the effective Hamiltonian of the interaction,

$$H=\int_V d^3r\,\chi(\vec{r})E_p^{(-)}(\vec{r})E^{(+)}(\vec{r})E^{(+)}(\vec{r})+\text{H.c.} \quad (2.1)$$

Here $E_p$ is the pump field, which is assumed to be classical and monochromatic, and $E$ is the operator of the scattered field. In the first order of perturbation theory, the quantum state of the scattered light has the entangled form

$$|\Psi\rangle=|\text{vac}\rangle+\sum_{kk'}F(\vec{k},\vec{k}')|1\rangle_k|1\rangle_{k'}, \quad (2.2)$$

$$F(\vec{k},\vec{k}')=\int_V d^3r\,\chi(\vec{r})E_p^{(-)}(\vec{r})\exp[i\vec{\Delta}(\vec{k},\vec{k}')\cdot\vec{r}], \quad (2.3)$$

$$\omega(\vec{k})+\omega(\vec{k}')=\omega(\vec{k}_p), \quad (2.4)$$

$$\Delta(\vec{k},\vec{k}')=\vec{k}+\vec{k}'-\vec{k}_p. \quad (2.5)$$

Here $E_p(\vec{r})$ is the slowly varying pump amplitude [without the factor $\exp(ikz)$]. Since we are only interested in the form of the PS spectrum, hereafter we omit unimportant constants. The probability of a coincidence between photocounts of two detectors selecting the modes $\vec{k}$ and $\vec{k}'$ is

$$P_c(\vec{k},\vec{k}')=|F(\vec{k},\vec{k}')|^2. \quad (2.6)$$

To calculate the probability $P_1(\vec{k})$ of a photocount from a single narrow-band detector, the expression above should be integrated over all unregistered (''idler'') modes $\vec{k}'$:

$$P_1(\vec{k})=\int d^3k'\,P_c(\vec{k},\vec{k}'). \quad (2.7)$$

This is a typical relation between marginal and full probability distributions.

Let the scattering region have a shape of a layer with thickness $l$, perpendicular to the pump wave vector $\vec{k}_p$. Let also all three wave vectors $\vec{k}$, $\vec{k}'$, and $\vec{k}_p$ lay in the same plane $(x,z)$ (the $x$ axis is directed along the layer, the $z$ axis is parallel to the $\vec{k}_p$). Let the function $f(x)\equiv\chi(x)E_p(x)$ describe slow variation of nonlinearity and/or of the pump amplitude. The function $\chi(x)$ describes possible variation of the nonlinearity in the transverse direction (e.g., because of the

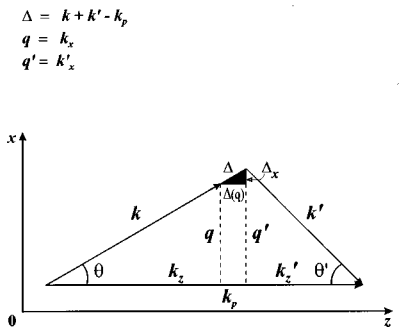


FIG. 3. A scheme illustrating the geometry of scattering and other necessary notation.

domain structure of the crystal [22]), and the function $E_p(x)$ describes the amplitude profile of the pump beam in the near field zone. In our experiments, $l/k_p a^2 \ll 1$ ($a$ is the typical transverse size of the pump beam or of the crystal inhomogeneities), so the effects of transverse nonuniformness of the crystal [''the nonlinear diffraction and interference;'' see Fig. 1(b)] are indistinguishable from those of the pump beam nonuniformness.

Let the pump be extraordinary and both scattered waves be ordinary rays of the crystal. Then $k(\omega)=n(\omega)\omega/c$, $k'(\omega)=n(\omega')\omega'/c$, $\omega'=\omega_0-\omega$ ($n$ is the refraction index). The scattered field wave vector $\vec{k}$ has two components: $k_x \equiv q<k$ and $k_z(\omega,q)=\sqrt{k^2(\omega)-q^2}>0$, so a mode is determined by two parameters, $\omega$ and $q$. Orientation of all wave vectors is shown in Fig. 3. The scattering angle inside the crystal is $\theta=\tan^{-1}[q/k(\omega)]$. We will be interested in the angular structure of the coincidence probability and single detection probability at some fixed frequency $\omega$. Then using Eqs. (2.3), (2.6), and (2.7) we get

$$P_c(q,q')=|F(q,q')|^2, \quad P_1(q)=\int dq' P_c(q,q'),$$

$$F(q,q')=F_x(q,q')F_z(q,q'),$$

$$F_x(q,q')=\int dx f(x)\exp[i(q+q')x],$$

$$F_z(q,q')=\mathrm{sinc}[\Delta_z(q,q')l/2], \quad f(x)\equiv\chi(x)E_p(x). \tag{2.8}$$

Let us consider three typical cases.

(1) For a uniform crystal and a Gaussian pump $f(x) \propto \exp(-x^2/a^2)$, so

$$F_x(q,q')=\exp[-(q+q')^2a^2/4]. \tag{2.9}$$

This function has considerable magnitude only when $|q+q'|\leqslant 1/a$.

(2) For two crystals placed parallel to the pump beam as in Fig. 1(b), the function $f(x)$ can be assumed to differ from zero only in two intervals: $(b-a)/2<x<(b+a)/2$ and $-(b-a)/2<x<-(b+a)/2$ (now $a$ is the transverse size of the crystals and $b$ is the distance between their centers, $b>a$). Then

$$F_x(q,q')=\mathrm{sinc}[(q+q')a/2]\cos[(q+q')b/2]. \tag{2.10}$$

The above result is also valid in the case when the pump is diffracted by a double-slit screen placed right in front of a single wide crystal: effect of the functions $\chi(x)$ and $E_p(x)$ is the same provided $l \ll k_p a^2$.

(2a) If the nonlinearities in the two crystals have opposite signs, $\chi_1=-\chi_2$, (or if a phase delay $\pi$ is inserted into the pump beam in front of one slit), then the interference pattern is shifted by $\pi$:

$$F_x(q,q')=\mathrm{sinc}[(q+q')a/2]\sin[(q+q')b/2]. \tag{2.11}$$

Now the scattering in the exact transverse matching direction $q+q'=0$ is suppressed.

(3) For $\chi(x)$ periodically modulated because of the layer-type polydomain structure of the crystal [22], the first harmonic is $\chi(x)\propto\cos(Kx)$, so that

$$F_x \approx \delta(q+q'+K)+\delta(q+q'-K) \tag{2.12}$$

(in the experiments [22], each two neighboring domains had opposite signs of $\chi$, so $K=\pi/d$, where $d$ is domain thickness).

The angular structure of the spectrum caused by the transverse nonuniformness $f(x)$ may be smoothed by the function $F_z(q,q')$. This effect depends on the layer length $l$ and the scattering angles $\theta,\theta'$. The longitudinal wave detuning is

$$\Delta_z(\omega,q,q')=k_z+k_z'-k_p = \sqrt{k^2(\omega)-q^2}+\sqrt{k^2(\omega')-q'^2}-k_p. \tag{2.13}$$

We will expand linearly the longitudinal wave detuning near the exact matching point $\Delta_z(\omega,q_0,-q_0)=0$ for a fixed frequency $\omega$. Let

$$q_0(\omega)\equiv q_0=k_{0z}\tan\theta_0=k'_{0z}\tan\theta'_0\geqslant 0, \quad \theta\ll 1, \quad \theta'\ll 1,$$

$$k_{0z}\equiv\sqrt{k^2-q_0^2}\geqslant 0, \quad k'_{0z}\equiv\sqrt{k'^2-q_0^2}\geqslant 0,$$

$$k_p=k_{0z}+k'_{0z}, \tag{2.14}$$

then

$$\Delta_z(\omega,q_0,q_0)\approx C_\omega(\omega-\omega_0)-C_q(q-q_0)+C_{q'}(q'+q_0),$$

$$C_\omega=[1/u_z-1/u'_z]_0,$$

$$C_q=\tan\theta_0, \quad C_{q'}=\tan\theta'_0. \tag{2.15}$$

Here $u_z=u\cos\theta$ and $u=d\omega/dk$ is the group velocity. Then we find the effective widths of the function $F_z$ with respect to its three arguments:

$$\Delta\omega_l=2\pi\lambda|C_\omega|l, \quad \Delta q_l=2\pi\lambda C_q l, \quad \Delta q'_l=2\pi\lambda C'_q l. \tag{2.16}$$

Note that $C_\omega l$ has a simple meaning. It is the time difference of the signal and idler photons traveling through the layer $l$ (in experiment, the frequency is usually measured not at a

fixed $\theta$ but at a fixed external scattering angle $\Theta$; the following corrections are usually inessential).

Let us subsequently consider the conditions for the observation of PS diffraction and interference by one and two detectors.

### A. Fourth-order interference

Let the frequency $\omega$ and one of the directions $q'=-q_0$ be fixed (and belong to the phase matching region), and the coincidence rate be measured as a function of the direction $q$, that is, of the transverse coordinate of the signal detector. Then it follows from Eq. (2.8) that

$$F(q)\equiv F(q,-q_0)=F_x(q)F_z(q),$$

$$F_x(q)=\int dx f(x)\exp[i(q-q_0)x],$$

$$F_z(q)=\mathrm{sinc}[\Delta(q)l/2], \tag{2.17}$$

where

$$\Delta(q)\equiv\Delta_z(q,-q_0)=k_z(q)+k'_{0z}-k_p=\sqrt{k^2-q^2}-k_{0z}. \tag{2.18}$$

In the linear approximation, $\Delta(q)=-\tan\theta_0(q-q_0)$ (see Fig. 3), so

$$F_z(q)\approx\mathrm{sinc}[(q-q_0)l\ \tan\ \theta_0/2]=\mathrm{sinc}[\pi(q-q_0)/\Delta q_l]. \tag{2.19}$$

The observed angular dependence of the coincidence probability $P_c(q)=|F(q)|^2$ is defined by the product of two functions: $F(q)=F_x(q)F_z(q)$. There are two extreme cases.

(A) Let the following condition hold:

$$\epsilon\equiv l\ \tan\ \theta_0/a\ll 1, \tag{2.20}$$

where $a$ is a typical length of nonuniformness along the $x$ axis (i.e., either small scattering angles for the signal radiation observed by the movable detector, or a short crystal). Then the function $F_z$ is close to unity whenever $F_x$ has significant value, and hence

$$F(q)\approx F_x(q)=\int dx f(x)\exp[i(q-q_0)x], \tag{2.21}$$

that is, the angular spectrum of the scattering matrix is defined by the Fourier transform of the function $f(x)\equiv\chi(x)E_p(x)$. This effect can be called nonlinear diffraction or nonlinear interference [22]; $\epsilon\ll 1$ can be interpreted as the condition for the signal photons not to cross the transverse inhomogeneities of the scattering volume. There is no restriction on the scattering angles for idler photons (registered by the fixed detector).

If $\chi(x)=\mathrm{const}$, the Fourier transform of $f(x)$ is the $k_x$ spectrum of the pump. It may be defined by an object inserted into the pump beam (a two-slit mask in our *nonlinear Young's experiment*).

(B) Let $\epsilon\gg 1$ (large scattering angles or long crystal; the signal photons do cross the inhomogeneities whose role is thus averaged). Then $F(q)\approx F_z(q-q_0)=\mathrm{sinc}[\pi(q-q_0)/\Delta q_l]$, that is, the observed width of the resonance will be determined by the length of the crystal, $\Delta q=\Delta q_l$. The transverse nonuniformness of the scattering region does not matter.

Therefore, the structure of the angular dependence $P_c(q)$ is mainly determined by the narrowest of the functions $F_x(q)$ or $F_z(q)$ (if the difference is significant), and hence the condition required to observe interference or diffraction by the coincidences method [the scheme in Fig. 2(b)] is $\epsilon\ll 1$ (small signal scattering angles and/or short crystals).

### B. Second-order interference

Now let us study the angular shape of the signal using a single detector (with narrow angular and frequency band around $q_0,\omega$). The coincidence probability has to be integrated over all idler modes, which are nonobservable now; see Eq. (2.8):

$$P_1(q)=\int dq'|F_x(q,q')F_z(q,q')|^2. \tag{2.22}$$

The scales of $F_x$ and $F_z$ variations as functions of $q'$ are of the order of $1/a$ and $1/l\theta'$, respectively, so again we have two extreme cases. However, in order to observe diffraction, now we need to use large angles $\theta'$ of the idler wave scattering.

(A) Let

$$\epsilon'\equiv l\ \tan\ \theta'_0/a\ll 1 \tag{2.23}$$

(small scattering angles of the ''central'' idler wave conjugated to the signal). Then the dependence of $F$ on $q'$ for a fixed $q$ is again determined mainly by the most ''narrow'' function $F_x$. Now, however, its structure is ''washed away'' by integrating over $q'$, and the observed line shape is determined by a more wide function $F_z$. In other words, the more narrow function $F_x$ plays the role of delta function while integrating over $q'$: $F_x(q,q')\approx\delta(q+q')$, and its shape does not influence the observable angular structure.

As an example, let us consider the above case (2.9) with a uniform crystal and a Gaussian pump. For $l\ \tan\theta'_0\ll a$, we can substitute $q'\approx -q$ into more slow functions $\Delta_z(q,q')$ and $F_z$:

$$\Delta_z(q,q')\approx\Delta_z(q,-q)\equiv\Delta_z(q)=\sqrt{k^2-q^2}+\sqrt{k'^2-q^2}-k_p,$$

$$F_z(q,q')\approx F_z(q,-q)\equiv F_z(q)=\mathrm{sinc}[\Delta_z(q)l/2]. \tag{2.24}$$

As a result, the diffraction structure is ''smoothed:''

$$P_1(q)\approx\mathrm{sinc}[\Delta_z(q)l/2]. \tag{2.25}$$

One can say in this case that the transverse momentum of the field is conserved for an elementary three-photon interaction, $k_x \approx -k_x'$, and the finite width of the angular resonance is due to nonconservation of the longitudinal momentum. Linear expansion near the exact phase matching direction, $\Delta_z(q)=0$, yields

$$\Delta_z(q) = -D_q(q-q_0),$$

$$D_q = \tan\,\theta_0 + \tan\,\theta_0' = q_0/k_{0z} + q_0/k_{0z}' = q_0 k_p/k_{0z}k_{0z}'. \tag{2.26}$$

The dependence on the scattering angle is

$$\Delta_z(q) = -D_\theta(\theta-\theta_0), \quad D_\theta = k_p\,\tan(\theta_0'). \tag{2.27}$$

The effective linewidth is found from the condition $\Delta_z l = 2\pi$:

$$\Delta q' = \frac{2\pi}{D_q l}, \quad \Delta\theta' = \frac{2\pi}{D_\theta l} = \frac{2\pi}{k_p l\,\tan(\theta_0')}. \tag{2.28}$$

*Thus PS diffraction is not observable by the one-detector method of registration for small scattering angles or short crystals, in contrast to the coincidence method of registration.*

(B) Now let $\epsilon' = l\,\tan\theta_0'/a \gg 1$ (long crystal and/or large scattering angles), so the function $F_x(q')$ is wider than the function $F_z(q')$. Consequently, $q'$ may be replaced by the function

$$Q'(q) \equiv -\sqrt{k'^2-(k_p-k_z)^2} = -\sqrt{k'^2-[k_p-\sqrt{k'^2-q^2}]^2}, \tag{2.29}$$

which is found from the equation $\Delta_z(q,Q'(q))=0$. Equation $\Delta_z=0$ may be called the condition of ''longitudinal'' or ''Cherenkov's'' matching. Now,

$$F_z(q,q') \propto \delta(\Delta_z(q,q')) \propto \delta(q'-Q'(q)) \tag{2.30}$$

and

$$P_1(q) = \left| \int dx f(x) \exp[i(q+Q'(q))x] \right|^2. \tag{2.31}$$

Linear expansion near the exact phase matching gives

$$F_z(q,q') \propto \delta(\Delta_z(q,q')) \propto \delta(\tan\,\theta_0(q-q_0) - \tan\,\theta_0'(q'+q_0)). \tag{2.32}$$

From Eq. (2.32) we find $q+q' = \eta(q-q_0)$, where $\eta \equiv 1 + k_{0z}'/k_{0z} = k_p/k_{0z} > 1$. As a result,

$$P_1(q) = \left| \int dx f(x) \exp[i(q-q_0)\eta x] \right|^2 = \left| \int dx f(x/\eta) \exp[i(q-q_0)x] \right|^2. \tag{2.33}$$

Thus, the single-detector angular line shape $P_1(q)$ is proportional to the Fourier transform of the profile $f(x/\eta)$, that is, it repeats the usual diffraction pattern of a plane wave in case of a screen with the transmission function $f(x)$, however, with the scaling coefficient $\eta > 1$ reducing the observable range of angles.

*The conclusion is that to observe interference according to Fig. 2(b) by a single detector, long crystals and/or large scattering angles of the idler (not observed) photons are needed.* The inequality $\epsilon' \gg 1$ can be interpreted as a requirement for the idler photons to cross transverse nonuniformnesses of the scattering volume. This erases the ''which domain'' information and enables interference. *Therefore, the overlap of the* idler *wave packets from two distinguishable macroscopic domains results in interference of* signal. *In this way, the biphoton properties still play an important role in experiment involving the single-photon (as opposed to coincident) detections.*

Let us turn to the scattering angle $\theta$. From $q = k\,\sin\,\theta$ it follows that $dq = k_{0z}d\theta$, so the angular line shape inside the crystal is

$$P_1(\theta) = \left| \int dx f(x) \exp[i(\sin\,\theta - \sin\,\theta_0)kx\eta] \right|^2 \approx \left| \int dx f(x) \exp[i(\theta-\theta_0)k_p x] \right|^2. \tag{2.34}$$

Taking refraction into account, we obtain the connection $q = (\omega/c)\sin\Theta$, so that $dq = (\omega/c)\cos\Theta_0 d\Theta$, where $\Theta$ is the external scattering angle. The observed angular line shape takes the form

$$P_1(\Theta) = \left| \int dx f(x) \exp[i(\sin\,\Theta - \sin\,\Theta_0)\omega\eta x/c] \right|^2 \approx \left| \int dx f(x) \exp[i(\Theta-\Theta_0)\omega x\eta\,\cos\,\Theta_0/c] \right|^2. \tag{2.35}$$

Usual diffraction of the pump on the amplitude profile $f(x)$ in vacuum gives the angular distribution

$$\left| \int dx f(x) \exp[iq_p x] \right|^2 = \left| \int dx f(x) \exp[i\Theta\omega_p x/c] \right|^2, \tag{2.36}$$

so the observed angular structure of a PS diffraction pattern at frequency $\omega$ is only different from diffraction of the pump on the same profile by an angular shift $\Theta_0$, and by a close to unity scaling factor

$$\omega\eta\,\cos\,\Theta_0/\omega_p = n_p\,\cos\,\Theta_0/n_\omega\,\cos\,\theta_0. \tag{2.37}$$

The result (2.37) has a trivial geometric explanation: transverse nonuniformness of the interaction is equivalent to a certain distribution of the pump wave vector directions; direction of the signal is linked to the pump direction by the ''phase matching triangle'' $\vec{k}+\vec{k}' = \vec{k}_p$, so the angular spectrum of the pump is reproduced by that of the signal.

We also stress that the angular line shape of the scattered radiation is of a three-frequency interference type: phase delays introduced into any of the three modes $\vec{k}$, $\vec{k}'$, or $\vec{k}_p$ will change the interference pattern (both in the second and fourth order).

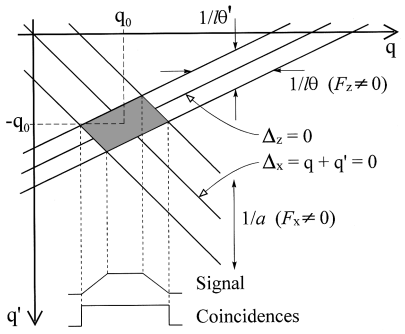


FIG. 4. Geometrical illustration of observation conditions for the second- and the fourth-order interference in the space of wave vectors. For simplicity, we suppose here that the functions $F_z(\Delta_z)$, $F_x(\Delta_x)$ have rectangular profiles along the directions of $\vec{q}$ and $\vec{q}'$.

Note that if the pump is extraordinary and the optic axis $C$ of the crystal lies in the plane of diffraction $(xz)$, then a sort of ''amplification'' of interference is observed. This effect is caused by the dependence of $k_p$ on the direction and the corresponding change of the tuning curve. It is most noticeable in the degenerate case when collinear phase matching takes place for the frequency $\omega_0=\omega_p/2$. For this reason, in all experiments the geometry was chosen so as to avoid this effect, that is, $C$ did not belong to $(xz)$.

Thus, there is a complementarity of conditions for the observation of Young's three-frequency interference using one $(\epsilon'\gg 1)$ and two $(\epsilon\ll 1)$ detectors (a similar type of complementarity was obtained from general considerations [28]). It can be illustrated by a simple geometric interpretation (Fig. 4). Geometric sizes $a$ and $l$ of the scattering region determine the set of allowed wave vectors in the space $\vec{k}\otimes\vec{k}'$. For these vectors,

$$|\Delta_x|\leqslant 1/a, \quad |\Delta_z|\leqslant 1/l \tag{2.38}$$

[in two-dimensional case and for the simplest distribution $f(x)$ when the pump is constrained by the aperture $a$]. The frequencies $\omega$, $\omega'$ and hence the wave vectors $k=n\omega/c$, $k'=n'\omega'/c$ are assumed to be fixed.

Figure 4 shows the region of allowed wave detunings $\Delta_z$ and $\Delta_x$ for $F_z$ and $F_x$. The cross section of the shadowed parallelogram in the direction parallel to the $q$ axis determines the angular width of the signal $P_1(\Theta)$ and coincidences $P_c(\Theta)$.

## III. THREE-FREQUENCY MACH-ZEHNDER INTERFEROMETER

Let the scattering volume be uniform in the $(x\text{-}y)$ plane (diffractionless approximation, $a\gg l\tan\theta_0$, $a\gg l\tan\theta_0'$), then the modes are bound strictly in pairs: conjugate modes are uniquely determined by the conditions of stationarity and transverse uniformness:

$$\omega'=\omega_p-\omega, \quad k_x'=-k_x, \quad k_y'=-k_y,$$

$$k_z'=\sqrt{k^2(\omega_p-\omega)-k_x^2-k_y^2}. \tag{3.1}$$

If linear optical properties (dispersion) are uniform in all volume, but the nonlinearity $\chi(z)$ is arbitrarily distributed along the $z$ axis (parallel to the pump wave vector $\vec{k}_p$), then our model describes parametric scattering in a multiply layered crystal with the pump propagating orthogonally to the boundaries of all domains. In a two-dimensional model, the probability amplitude of a photon pair birth in the modes $(\omega,q)$ and $(\omega',-q)$ (here $q\equiv k_x=-k_x'$) is, according to Eqs. (2.3), (2.13),

$$F(\omega,q)=\int dz\chi(z)\exp[i\Delta(\omega,q)z], \tag{3.2}$$

$$\Delta_z(\omega,q)=k_z+k_z'-k_p=\sqrt{k^2(\omega)-q^2}+\sqrt{k^2(\omega')-q^2}-k_p. \tag{3.3}$$

In the linear approximation,

$$\Delta_z(\omega,q)=C_\omega(\omega-\omega_0)-C_q(q-q_0), \tag{3.4}$$

where

$$C_\omega=[1/u_z-1/u_z']_0,$$

$$C_q=\tan\theta_0-\tan\theta_0'=q_0(1/k_{0z}-1/k_{0z}'). \tag{3.5}$$

In the above expressions $u_z=u\cos\theta$, $u=d\omega/dk$ is the group velocity. Now Eq. (3.2) takes the form

$$F(\omega,q)=\int dz\chi(z)\exp\{i[C_\omega(\omega-\omega_0)-C_q(q-q_0)]z\}. \tag{3.6}$$

Thus the frequency line shape $P_1(\omega,q_0)=|F(\omega,q_0)|^2$ observed at a fixed angle $\theta=\theta_0$ is determined by the Fourier transform of the nonlinearity distribution $\chi(z)$. This allows us to study the domain structure of nonlinear crystals. If the distribution is uniform over the length $l$ we obtain the spectrum of a pulse with rectangular envelope:

$$P_1(\omega,q_0)=\mathrm{sinc}^2[\pi(\omega-\omega_0)/\Delta\omega_l], \tag{3.7}$$

where $\Delta\omega_l=2\pi/|C_\omega|l$ is the effective frequency linewidth.

Now let us have two similar nonlinear layers of thickness $l$ separated by a transparent substance with thickness $l_1$ [Fig. 2(b)]. It follows from Eq. (3.2) that

$$F(\omega,q)=\mathrm{sinc}(\delta/2)\cos((\delta+\delta_1)/2). \tag{3.8}$$

(We replaced $\Delta_z$ by $\Delta_{1z}$ while integrating over the gap between the crystals.) In Eq. (3.8)

$$\delta\equiv\Delta_z(\omega,q)l, \quad \delta_1\equiv\Delta_{1z}(\omega,q)l_1,$$

$$\Delta_{1z}(\omega,q)=k_{1z}+k_{1z}'-k_{1p}=\sqrt{k_1^2(\omega)-q^2}+\sqrt{k_1^2(\omega')-q^2}-k_{1p}. \tag{3.9}$$

Here $k_1(\omega)=n_1(\omega)\omega/c$ is the dispersion of the intermediate layer; conservation of the transverse component $q$ while the light is refracted at the layers' boundaries is also taken into account. The first factor in Eq. (3.8) describes a usual scattering in a single layer $l$, the second one describes some additional frequency-angular structure due to the interference of spontaneous radiation from two layers; see Figs. 6 and 7. If $l_1=0$, expression (3.8) reduces to $F=\mathrm{sinc}(\delta/2)$, describ-

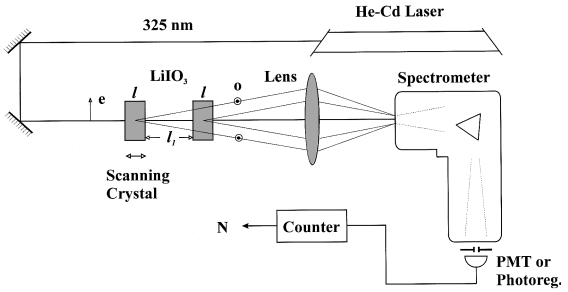


FIG. 5. Experimental setup for the observation of nonlinear second-order Mach-Zehnder interference.

ing scattering by a layer with double thickness $2l$. This is analogous to Ramsey's interference in the spectroscopical method of separated beams [18]. The expression (3.8) as well as (2.10) is the Fourier transform of two segments of sine, that is, an oscillator response to two resonant pulses with rectangular envelopes.

Let us consider a particular case of collinear phase matching, $q_0=0$, for the degenerate frequency $\omega_0=\omega_p/2$. This case corresponds to the crystal orientation for second harmonic generation. The frequency-angular spectrum of the field scattered to the region adjoint to $(\omega_0,q_0)$ has a specific shape of a ''cross,'' see Figs. 6(a),(b) and Fig. 7 below. We pass to external scattering angles, which are assumed to be small:

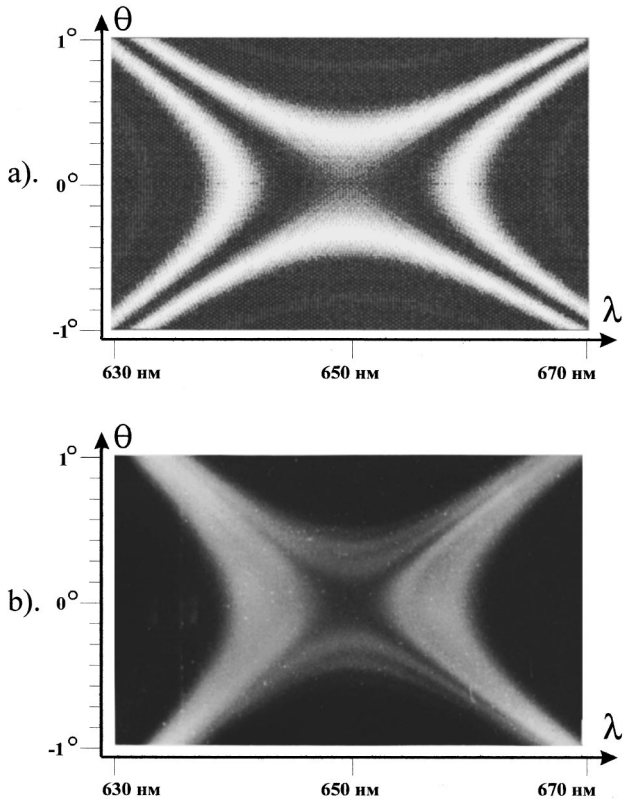


FIG. 6. Nonlinear second-order Mach-Zehnder interference. The separation of two $LiIO_3$ crystals of length $l$ is $l_1=0$. Polar axes of the two crystals are directed oppositely. (a) Calculated frequency-angular intensity distribution of signal radiation. (b) Photograph of frequency-angular intensity distributions near degenerate phase matching.

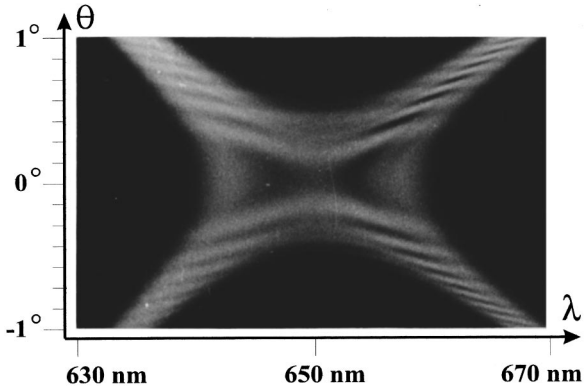


FIG. 7. The same as in Fig. 6(b) but for $l_1=10$ mm.

$$q=k\ \sin\ \theta=\omega\ \sin\ \Theta\approx\omega\Theta \tag{3.10}$$

(we put $c=1$). Keeping the second-order terms in $\Omega\equiv\omega-\omega_0$ and $\Theta$, we have

$$k_z(\Omega,\Theta)=\sqrt{k^2(\omega)-\omega^2\Theta^2}\approx k_{0z}+\Omega/u_0+A\Omega^2-B\Theta^2,$$

$$k_z'(\Omega,\Theta)=k_z(-\Omega,\Theta),$$

$$\Delta_z(\omega,\Theta)=A\Omega^2-B\Theta^2. \tag{3.11}$$

In Eq. (3.11),

$$A\equiv\left[\frac{d^2k}{d\omega^2}\right]_0=2\left[\frac{dn}{d\omega}\right]_0+\omega_0\left[\frac{d^2n}{d\omega^2}\right]_0,$$

$$B\equiv\frac{\omega_0}{n_0},\quad k_p=2k_{0z}. \tag{3.12}$$

Thus the frequency-angular spectrum of scattering around the ''cross'' region in a single crystal is [cf. Eq. (3.7)]

$$P_1(\Omega,\Theta)=\mathrm{sinc}^2[(A\Omega^2-B\Theta^2)l/2]. \tag{3.13}$$

The slope of the tuning characteristics, frequency and angular linewidths at the center of the ''cross'' $(\omega_0,q_0)$ are

$$\frac{d\Theta}{d\omega}=\sqrt{\frac{A}{B}},\quad \Delta\omega=C\sqrt{\frac{2}{Al}},\quad \Delta\Theta=C\sqrt{\frac{2}{Bl}}, \tag{3.14}$$

respectively. In Eq. (3.14), $C\equiv4\sqrt{\pi/3}=2.363$ is the integral of the function $\mathrm{sinc}^2(x^2)$ in infinite limits. The full width at half maximum and the effective (with respect to the area) width of the function $\mathrm{sinc}^2(x^2)$ are nearly the same. For our experiment, which is described below,

$$\lambda_0=2\pi/\omega_0=0.65\ \mu\mathrm{m},\quad n_0=1.88,$$

$$A/2\pi=0.151\ \mu\mathrm{m},\quad 2\pi B=0.818\ \mu\mathrm{m}^{-1}, \tag{3.15}$$

$$\Delta\nu=\Delta\omega/2\pi=0.028\ \mu\mathrm{m}^{-1},\quad \Delta\Theta=0.69°,$$

$$d\Theta/d\nu=24.6\ \mathrm{deg}\ \mu\mathrm{m}. \tag{3.16}$$

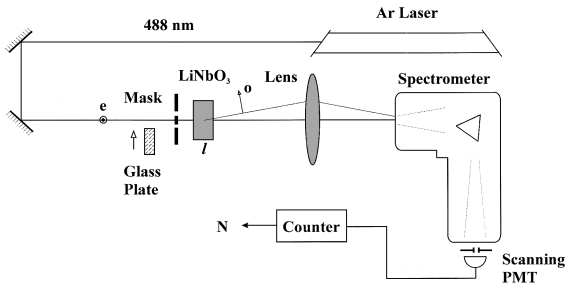


FIG. 8. Experimental setup for the observation of Young nonlinear second-order interference.

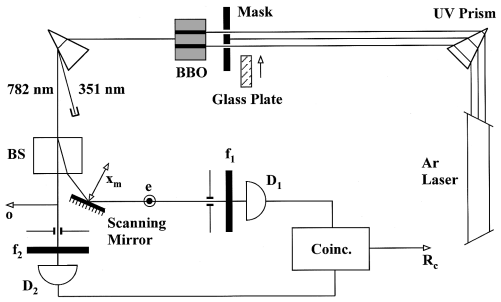


FIG. 9. Experimental setup for the observation of fourth-order nonlinear Young interference.

If two similar crystals are separated by a vacuum gap $l_1$, the ''cross'' displays a fine interference structure (Fig. 7). The structure is described by expression (3.8) where, likewise (3.11) and (3.12),

$$k_{1z}(\Omega,\Theta)=\sqrt{\omega^2-\omega^2\Theta^2}\approx\omega_0+\Omega-\omega_0\Theta^2/2,$$

$$k'_{1z}(\Omega,\Theta)=k_{1z}(-\Omega,\Theta),\quad \Delta_{1z}(\Omega,\Theta)\approx-\omega_0\Theta^2, \tag{3.17}$$

for $n=1$. Expressions (3.8), (3.12), and (3.17) were used to draw the diagram in Fig. 6(a); see below. Let $\Omega$ and $\Theta$ be connected by the phase-matching conditions $\Delta_z(\omega,\Theta)=0$, i.e., $\pm\Theta_0(\Omega)=\pm(d\Theta/d\omega)\Omega$. The signal intensity shows beating according to Eq. (3.8):

$$P_1(\Theta_0(\Omega))\propto\cos^2(\Delta_{1z}l_1/2)=\cos^2(\omega_0\Theta^2 l_1/2). \tag{3.18}$$

The signal vanishes when

$$\Theta_m=\sqrt{m\pi/\omega_0 l_1}=\sqrt{m\lambda_0/2l_1}=0.33^\circ\sqrt{m},\quad m=1,3,\ldots. \tag{3.19}$$

When the two crystals have opposite directions of polar axes, the cosine in Eq. (3.18) is replaced by sine, so the minima happen at

$$\Theta'_m=\sqrt{m\lambda_0/l_1}=0.46^\circ\sqrt{m},\quad m=0,1,2,\ldots. \tag{3.20}$$

According to Eq. (3.14), the ratio of the first minima position $\Theta'_1$ and the half-width of the line in the center is

$$\frac{2\Theta'_1}{\Delta\Theta}=\frac{3}{2}\sqrt{\frac{l}{n_0 l_1}}=1.33. \tag{3.21}$$

These theoretical conclusions are in good agreement with the experimental results given below.

## IV. EXPERIMENT

Three versions of the experimental setup have been used to observe the interference: (1) two scattering regions perpendicular to the pump wave vector; registration by a single detector (Fig. 8); (2) the same, registration by two detectors (method of coincidences, Fig. 9); and (3) two vacuum separated regions along the pump; registration by a single detector (Fig. 5).

### A. Nonlinear Young's second-order interference

The experimental setup is shown in Fig. 8. Two scattering regions were obtained by using a screen with two slits placed directly in front of the nonlinear crystal (lithium niobate doped by 5% of MgO). We used two screens (masks) with different sizes: (1) Mask 1, $a=0.082$ cm, $b=0.192$ cm; (2) Mask 2, $a=0.212$ cm, $b=0.400$ cm. The crystal length was $l=1.05$ cm. The pump was argon laser radiation (power 3 W, $\lambda_p=0.488$ $\mu$m, divergence $2\times10^{-4}$ rad, beam radius 1 mm). The radius of coherence was also about 1 mm. The signal radiation with wavelength $\lambda$ was registered in the range 0.54–0.7 $\mu$m either photographically or by a photoelectronic scanning system. The corresponding idler waves spectrum ranged from 5 to 1.6 $\mu$m (the upper polariton branch) where $LiNbO_3$ is still transparent. The type-I phase matching was used, with the signal and polariton waves polarized in the $x$ direction—normally to the optic axis ($o$ waves), and the pump polarized along $y$ and being an $e$ wave. The pump polarization was parallel to the slits ($y$ direction), i.e., the optic axis of the crystal lay in the $(y$-$z)$ plane and the diffraction occurred in the $(x$-$y)$ plane.

The signal radiation propagated through a lens and the input slit of a spectrograph placed in the focus of the lens, $F$. The input slit was parallel to the $y$ axis. This optical system provided a two-dimensional intensity distribution observed at the output of the spectrograph in coordinates wavelength $\lambda$ angle $\Theta$ (''crossed dispersion'') [14].

Figure 10 shows a snapshot of a part of the frequency-angular spectrum observed using mask 2, and Fig. 11 shows the angular line shape (obtained by scanning along the angular axis) at wavelength $\lambda=0.633$ $\mu$m, with mask 1. The theoretical curve (solid line) was found from Eq. (2.34). Its horizontal scaling was found from the links $x=C\Theta$ and $\Theta=\lambda q/2\pi$. The scaling coefficient $C\equiv dx/d\Theta=216\pm5$ mm/rad was measured by two methods that gave almost identical results: by the observation of the pump diffraction on the same slits, and by a HeNe laser beam diffraction on a Fabry-Pérot cavity. The only fitting parameters were the overall vertical and horizontal shift of the theoretical curve, and its vertical stretching. The dashed lines correspond to the calculated maxima positions on the diffraction curve at the pump wavelength ($x_1=\pm C\lambda_p/b=\pm0.55$ mm); the solid lines correspond to the same at the signal wavelength ($x_1=\pm C\lambda/b=\pm0.71$ mm). We see from the figure that the experiment confirms the theoretical prediction (2.34): for $\epsilon'\gg1$, nonlinear diffraction of the signal repeats (with a shift of $\pm\Theta_0=3.8^\circ$) a usual diffraction of the pump on two slits.

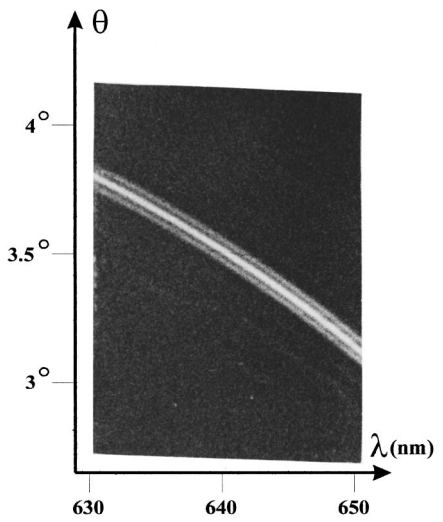


FIG. 10. Photograph of a fragment of the frequency-angular spectrum of spontaneous parametric down-conversion with double slit inserted in the pump. Parameters of the double slit are $a = 0.085$ cm and $b = 0.192$ cm.

Figure 12 shows analogous data in the case when a glass plate shifting the pump phase by $\pi$ was placed in front of one slit.

### B. Nonlinear fourth-order Young's interference

To register nonlinear diffraction by the method of coincidences, an argon laser with wavelength $\lambda_p = 0.351$ $\mu$m and a BBO crystal were used (Fig. 9). The laser power was 0.3 W, the pump beam radius was 0.1 cm, its radius of coherence was of the same order of magnitude. The slit widths were $a = 150$ $\mu$m, the distance between the slits was $b = 470$ $\mu$m, and the crystal length was $l = 3$ mm. The detectors quantum efficiency was about 30%. Data accumulation time was 200 sec. Coincidence resolution was 10 nsec. The type-II degenerate collinear phase matching was used: the signal radiation and the pump wave were extraordinary rays polarized vertically—parallel to the slits. The ordinary idler

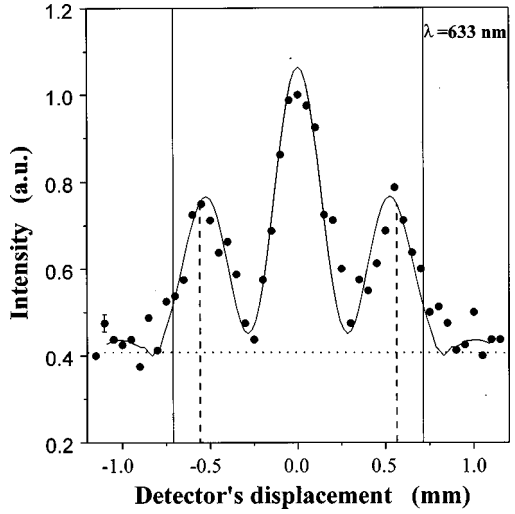


FIG. 11. Angular line shape of the signal radiation at $\lambda = 0.633$ mkm. In this case $a = 0.212$ cm and $b = 0.4$ cm.

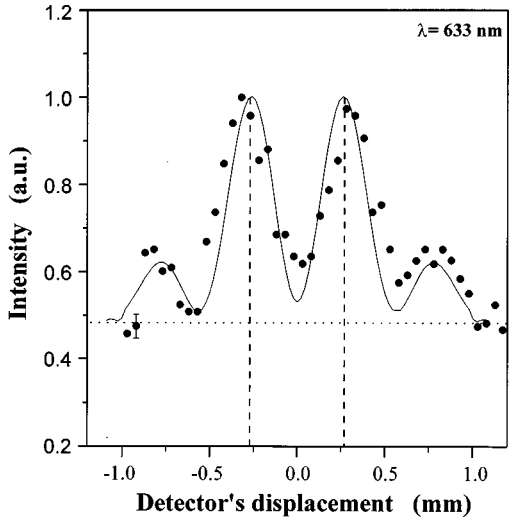


FIG. 12. The same as in Fig. 11 but with a glass plate shifting pump phase by $\pi$ placed in front of one slit.

wave was polarized along the horizontal axis $x$—normally to the slits. The wave vectors $\vec{k}$, $\vec{k}'$, and $\vec{k}_p$ were parallel, $\lambda = \lambda' = 2\lambda_p = 0.702$ $\mu$m. A polarizing beamsplitter BS placed after the crystal was used to separate the signal and idler modes in space. Similar interference filters $f_1$ and $f_2$ placed in front of the detectors $D_1$ and $D_2$ selected a narrow spectral band of about 3 nm around the degenerate frequency. Scanning of coincidences angular distribution was performed by an encoder driver which shifted a mirror in the signal channel, which is equivalent to scanning the detector. Pulses from the photodetectors were supplied to the input of the coincidence circuit. As a result, we obtained the coincidence number $R_c(x_m)$ registered during the accumulation time $t$ as a function of the position $x_m$ of the mirror. The equivalent shift of the detector was calculated as $x = 2x_m \sin\phi = 1.84x_m$, $\phi = 74°$.

Figure 13(a) shows the obtained $R_c(x)$ dependence. The theoretical curve (solid line) was calculated according to Eq. (2.21). Its horizontal scaling was found from the links $\Theta = \lambda q/2\pi$ and $x_m = C\Theta$, where $C \equiv dx_m/d\Theta = z/1.84 = 504$ mm/rad, and $z = 927$ mm is the distance between the crystal and the signal detector. The only fitting parameters were the overall vertical and horizontal shift of the theoretical curve, and its vertical stretching. The stretching procedure was carried out according to the relation $R_c(x_m) = R_c'(\lambda_m)/R_s(x_m)$, where $R_c'$ is the number of photocounts coincidences and $R_s$ the number of singles in the signal channel during the same time interval (200 sec). It was necessary to normalize the coincidences by $R_s$ because the finite detector aperture restricted the number of signal photocounts as we shifted the mirror. The dashed lines correspond to the calculated positions of the first additional maxima on the diffraction curve at the pump wavelength ($\Theta^* = \lambda_p/b = 0.74$ mrad, $x^* = \pm 0.68$ mm), the solid lines correspond to the same at the signal wavelength ($x = \pm 1.36$ mm). We see from the figure that the experiment confirms the theoretical prediction given by Eq. (2.21): for $\epsilon' \ll 1$ nonlinear diffraction observed by the coincidence method repeats usual diffraction of the signal on two slits.

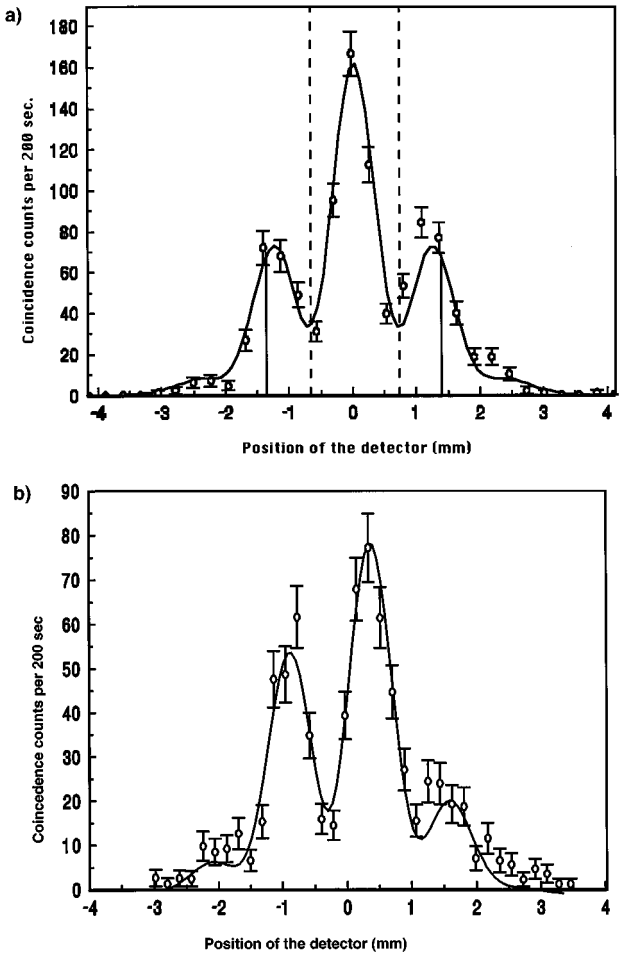


FIG. 13. Nonlinear fourth-order Young interference. The idler detector is fixed in the position of exact phase matching. The wavelengths are $\lambda=\lambda'=2\lambda_p=702$ nm. (a) Angular distribution of photocount coincidence rate with respect to the signal detector position. (b) The same but with a glass plate shifting the pump phase by approximately $\pi$ placed in front of one slit.

Figure 13(b) shows analogous data in the case where a glass plate shifting pump phase by approximately $\pi$ is placed in front of one slit.

### C. Nonlinear second-order Mach-Zehnder interference

For this type of interference, a HeCd laser operating at $\lambda_p=0.325\ \mu$m and two similar $LiIO_3$ crystals with $l=1.5$ cm were used (Fig. 5). The crystals were separated by a variable distance $l_1$. Their optical axes made an angle $\theta_p=59.2°$ with the pump wave vector $\vec{k}_p$ inside the crystal, and the scattering angle for the wave $\omega=\omega'=\omega_p/2$ was equal to zero, so the tuning curve had the shape of a cross (type-I phase matching). The crystals' optical axes were directed antiparallel, so that their effective quadratic susceptibilities had opposite signs $\chi_1=-\chi_2$. The optical scheme used for the collection of the scattered radiation was similar to the one described in Sec. IV A. Registration was performed photographically and by means of a detector scanned in the focal plane of the spectrograph.

The photograph obtained for $l_1=0$, together with the corresponding calculated diagram is shown in Figs. 6(a),(b).

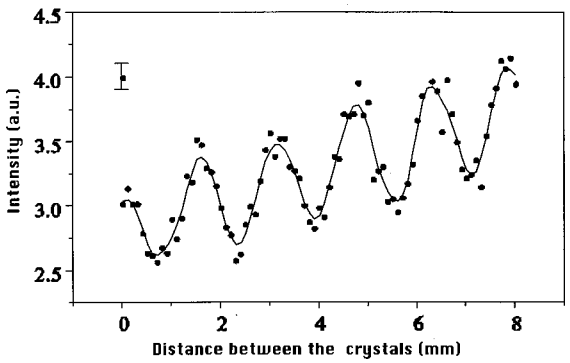


FIG. 14. Dependence of the signal intensity on $l_1$ at $\lambda=0.633\ \mu$m and scattering angle $\Theta=1.2°$.

Note the suppression of radiation in the directions and at the frequencies of the exact phase matching when the crystals are placed close to each other, $l_1=0$, and their polar axes have opposite directions, $\chi_1=-\chi_2$. Then the radiation from the first crystal is completely suppressed by the second one (and vice versa) in the directions of perfect phase matching. For $l_1\neq 0$, the frequency-angular spectrum has a complicated interference structure depending on $l_1$. In agreement with Eqs. (3.8) and (3.10), the distance between the maxima along the frequency and/or angular scale decreases as the air gap between the nonlinear crystals gets larger. Figure 7 demonstrates the interference distribution of the PS intensity when $l_1=10$ mm. In Fig. 14, the observed dependence of the signal intensity on the distance between two crystals at $\lambda=0.65\ \mu$m and at fixed scattering angle $\Theta=1.2°$. The oscillation period $\Delta l_1$ was found to be 1.6 mm, in a good agreement with calculations performed according to Eq. (3.8): $\Delta l_1=\lambda/\Theta^2=1.5$ mm. Note that according to Eq. (3.8), $\Delta l_1$ sharply depends on the scattering angle for given wavelength $\Theta(\lambda)$; that angle can be varied in the range of 0–10° by altering the angle $\theta_p$ of the crystal optical axis orientation with respect to the pump beam.

We would like to emphasize that the oscillation period is determined by the relative phase shift at all three frequencies $\phi+\phi'-\phi_p$ and turns out to be on the order of a millimeter. Therefore, these types of nonlinear interferometric schemes do not require precise tuning up to a wavelength.

## V. CONCLUSION

The experiments performed demonstrate possibilities for manipulating the structure of biphoton fields, based on the nonuniformness of the interaction region. They convincingly show that the simple model of PS effect applied here is quite adequate. This circumstance once again confirms that macroscopic quantum models can be used to describe spontaneous effects of nonlinear optics.

The observed diffraction and interference effects of parametric scattering in two nonlinear crystals may find a practical application for measurements of optical parameters, such as refraction and absorption, of optical materials by placing them between two crystals. In the above-developed theory, possible absorption at the signal and/or idler frequencies was not taken into account. As the idler frequency moves deeper into the IR range, its absorption should lead to

a decrease in the visibility of the observed interference and diffraction effects. This provides an opportunity to measure the absorption coefficient of nonlinear crystals in the polariton range. We have demonstrated here that the biphoton interference and diffraction is in some sense equivalent to the pump interference and diffraction. If a technical problem existed to build an interferometer for the pump in a medium that absorbs it but does not absorb the down-converted radiation, a two-photon interferometer would have been a solution.

## ACKNOWLEDGMENTS

A part of this work has been performed as a part of the programs ''Fundamental metrology. Multiphoton interferometry and its application for precise quantum measurements'' and was supported by Grant No. 96-02-16334a of the Russian Foundation for Basic Research. Strekalov and Shih thank the ONR of the U.S. for supporting the part of work done in the U.S.

[1] J. S. Bell, Physics (Long Island City, NY) **1**, 195 (1964); J. F. Clauser and A. Shimony, Rep. Prog. Phys. **41**, 1881 (1978); P. Grangier, M. J. Potasek, and B. Yurke, Phys. Rev. A **38**, 3132 (1988).

[2] Y. H. Shih and C. O. Alley, Phys. Rev. Lett. **61**, 2921 (1988); T. B. Pittman, Y. H. Shih, A. V. Sergienko, and M. H. Rubin, Phys. Rev. A **51**, 3495 (1995).

[3] A. V. Belinsky and D. N. Klyshko, Phys. Usp. **36**, 653 (1993).

[4] C. H. Bennet and S. J. Wiesner, Phys. Rev. Lett. **69**, 2881 (1992); A. K. Ekert, J. G. Rarity, P. R. Tapster, and G. M. Plama, *ibid.* **69**, 1293 (1992).

[5] J. D. Franson and H. Ilves, J. Mod. Opt. **41**, 2391 (1994).

[6] M. V. Chekhova, G. Kh. Kitaeva, S. P. Kulik, and A. N. Penin, Proc. SPIE **1863**, 192 (1993).

[7] D. N. Klyshko and A. N. Penin, Sov. Phys. Usp. **30**, 716 (1987); J. G. Rarity, K. D. Ridley, and P. R. Tapster, Appl. Opt. **26**, 4616 (1987); A. N. Penin and A. V. Sergienko, *ibid.* **30**, 3583 (1991); P. G. Kwiat, A. M. Steinberg, R. Y. Chiao, P. H. Eberhard, and M. D. Petrov, *ibid.* **33**, 1844 (1994).

[8] B. Ya. Zeldovich and D. N. Klyshko, JETP Lett. **9**, 40 (1969).

[9] C. K. Hong, Z. Y. Ou, and L. Mandel, Phys. Rev. Lett. **59**, 2044 (1987); A. M. Steinberg, P. G. Kwiat, and R. Y. Chiao, *ibid.* **68**, 2421 (1992); Y. H. Shih and A. V. Sergienko, Phys. Lett. A **186**, 29 (1994).

[10] D. N. Klyshko, Sov. Phys. Usp. **31**, 74 (1988).

[11] A. V. Belinsky and D. N. Klyshko, Laser Phys. **4**, 664 (1994).

[12] G. Kh. Kitaeva, D. N. Klyshko, and Ig. V. Taubin, Sov. Quantum Electron. **12**, 333 (1982); G. Kh. Kitaeva, A. N. Penin, and A. V. Sergienko, Dokl. Akad. Nauk SSSR **293**, 847 (1987).

[13] T. J. Herzog, J. G. Rarity, H. Weinfurter, and A. Zeilinger, Phys. Rev. Lett. **72**, 629 (1994).

[14] M. V. Chekhova, S. P. Kulik, and A. N. Penin, Opt. Commun. **114**, 301 (1995).

[15] T. B. Pittman, Y. H. Shih, D. V. Strekalov, and A. V. Sergienko, Phys. Rev. A **52**, R3429 (1995); T. B. Pittman, D. V. Strekalov, D. N. Klyshko, M. H. Rubin, A. V. Sergienko, and Y. H. Shih, *ibid.* **53**, 2804 (1996).

[16] A. N. Penin, T. A. Reutova, and A. V. Sergienko, *Workshop on Squeezed States and Uncertainty Relation*, NASA Special Publication No. 3135 (NASA, Greenbelt, MD, 1992), pp. 91–99.

[17] D. N. Klyshko, Phys. Lett. A **132**, 299 (1988).

[18] D. N. Klyshko, JETP **104**, 2676 (1993).

[19] D. N. Klyshko, JETP **105**, 1574 (1994).

[20] Z. Y. Ou, L. J. Wang, X. Y. Zou, and L. Mandel, Phys. Rev. A **41**, 566 (1990); X. Y. Zou, L. J. Wang, and L. Mandel, Phys. Rev. Lett. **67**, 318 (1991); Phys. Rev. A **44**, 4614 (1991).

[21] A. V. Belinsky and D. N. Klyshko, Phys. Lett. A **166**, 303 (1992).

[22] A. L. Alexandrovsky, G. Kh. Kitaeva, S. P. Kulik, and A. N. Penin, Sov. Phys. JETP **63**, 613 (1986).

[23] L. Hardi, Phys. Lett. A **161**, 362 (1992).

[24] A. Zeilinger, H. J. Bernstein, and M. A. Horn, J. Mod. Opt. **41**, 2375 (1994).

[25] L. J. Wang, X. Y. Zou, and L. Mandel, J. Opt. Soc. Am. B **8**, 978 (1991).

[26] B. Yurke, S. L. McCall, and J. R. Klauder, Phys. Rev. A **33**, 4033 (1986).

[27] J. D. Franson, Phys. Rev. Lett. **62**, 2205 (1989); Y. H. Shih and A. V. Sergienko, Phys. Rev. A **50**, 2564 (1994); P. H. S. Ribeiro, S. Padua, J. C. Machado, and G. A. Barbosa, *ibid.* **51**, 1631 (1995); T. S. Larchuk, M. C. Teich, and B. E. A. Saleh, *ibid.* **52**, 4145 (1995).

[28] G. Jaeger, A. Shimony, and L. Vaidman, Phys. Rev. A **51**, 54 (1995).